

Available online at www.sciencedirect.com**ScienceDirect**

Procedia Engineering 120 (2015) 912 – 915

**Procedia
Engineering**www.elsevier.com/locate/procedia

EUROSENSORS 2015

Impedance characterization of DNA-functionalization layers on AlGaIn/GaN high electron mobility transistors

N. Espinosa^{a,b,*}, S. U. Schwarz^{a,b}, V. Cimalla^b, A. Podolska^c and O. Ambacher^{a,b}^aDepartment of Microsystems Engineering, University of Freiburg, Georges-Köhler-Allee 106, 79110 Freiburg, Germany^bFraunhofer Institute for Applied Solid State Physics, Tullastr. 72, 79108 Freiburg, Germany^cAustralian Resources Research Centre, Curtin University, 26 Dick Perry Avenue, Kensington 6151, Western Australia

Abstract

Characterization and optimization for biosensor implementation with open gate AlGaIn/GaN transistors is described. Probe-DNA was immobilized on the gate. As target, complementary DNA at 10^{-12} - 10^{-7} mol/L was added. To investigate the impedimetric properties of the sensing area, electrochemical impedance spectroscopy was used. For very low frequencies, the bio-functionalization layer was modeled as a membrane with a charge transfer resistor in series with a Warburg element. This component presents impedance to diffusion of electrolyte ions. Its behavior is intermediate between a capacitor and a resistor (membrane impedance). After probe-target matching, the charge transfer resistance and Warburg impedance were increased (lower flow of electrolyte ions through the membrane). Using this working principle, a dynamic detection of targets is proposed.

© 2015 The Authors. Published by Elsevier Ltd. This is an open access article under the CC BY-NC-ND license (<http://creativecommons.org/licenses/by-nc-nd/4.0/>).

Peer-review under responsibility of the organizing committee of EUROSENSORS 2015

Keywords: GaN/AlGaIn HEMT; DNA layer characterization; charge transfer resistance; Warburg element; dynamic detection

1. Introduction

Nowadays, new biosensor technologies offer highly sensitive, cheap and miniaturized chips. A particular case is the application of open gate AlGaIn/GaN transistors [1]. Although these devices are highly sensitive, chemically stable and biocompatible, their potential for biosensing is usually not exploited using conventional methods. For example, very low change of the drain-source current is shown after addition of target molecules due to screening lengths of few nanometers [2, 3]. For improvement, deeper understanding regarding the insulator/biolyer interface

* Nayeli Espinosa. Tel.: +49-761-51-259; fax: +49-761-515-971-259.

E-mail address: nayeli.espinosa@iaf-extern.fraunhofer.de

is necessary, however, only few papers have modeled the sensing principle of DNA sensors with open gate silicon transistors [4-6]. They consider the DNA-layer as a perfect capacitor, which is uncertain for the following reasons: 1) Bilayers are non-uniform and should be modeled as porous membrane, where ions can penetrate; 2) Probe- and target-biomolecules have intrinsic charge (negative for DNA) and do not behave as a perfect dielectrics; and 3) Bio-functionalization layers are physical barriers with a resistance to ionic transfer and diffusion, especially at very low frequencies. The goal of this work is to clarify these mechanisms by electrochemical impedance spectroscopy (EIS), in order to take advantage of these properties. EIS is a powerful tool to investigate electrical and electrochemical properties of electrolyte/electrode interfaces. Here, the characterized sample acts as working electrode. A low amplitude AC voltage with a wide range of frequencies is applied as input, $U_{AC} = A_0 \sin(\omega t)$ with a typical amplitude of 5 mV. The input signal is the voltage between the working and reference electrodes. As output, the working electrode current is measured, $I_{out} = I_0 \sin(\omega t + \varphi)$. The presented experiments were performed without offset voltage. A linear relation between the reference electrode voltage and current from drain and source terminals was assumed.

Nomenclature

R	gas constant
T	temperature in Kelvin degree
F	Faraday constant
k	ion transfer rate constant
α	ion transfer coefficient
c_+, c_-	average concentration of positive or negative ions in the DNA layer
D_+, D_-	diffusion constant for positive or negative ions through the bilayer

2. Biosensor implementation

Transistors were fabricated on a heterostructure (120 nm AlN, 1800 nm GaN, 15 nm of $\text{Al}_{0.25}\text{Ga}_{0.75}\text{N}$, 6 nm GaN) grown by metal organic chemical vapor deposition on a SiC substrate and have a threshold voltage of -0.5 V. The gate surface was $400 \times 200 \mu\text{m}^2$. As bio-functionalization, probe-DNA was immobilized by a photochemical method [2]. Average probe density was $1.5 \times 10^{-13} \text{ cm}^{-2}$. As probe- and target-DNA, 5'-GCTT-ATCG-AGCT-TTCG-3' and 5'-CGAA-AGCT-CGAT-AAGC-3' were used. As electrolyte, 1 mmol/L phosphate buffered saline was added.

3. Results and interpretation

EIS demonstrates the insulator/electrolyte interface without DNA behaves close to a perfect capacitor (Figure 1a). Nonetheless, the insulator/DNA/electrolyte interface is modeled by a Randles circuit (Figure 1b), on which two types of currents flow (I_c and I_f). At high frequencies, I_c dominates and charges an imperfect double layer capacitor formed by an electrolyte diffuse layer and DNA molecules. For low and very low frequencies, a transport of ions through the DNA membrane occurs (I_f). This current is defined by a charge transfer resistor and Warburg element (membrane impedance to diffusion of ions). Since both elements presented a regular behavior at different target concentration, this work is focused in them. R_e is low and is neglected in both kinds of measurements. The charge transfer resistance depends on the ion concentration inside the membrane, for a monovalent electrolyte [7]:

$$R_{ct} = \frac{RT}{F^2 k (c_+)^{\alpha} (c_-)^{1-\alpha}} \quad (1)$$

The Warburg element considers accumulation of ions in a porous DNA layer. Its 45° phase represents an intermediate behavior between a resistor and a capacitor (Figure 1b). The resistive component is the electrolyte resistivity inside the bilayer cavities, whereas DNA molecules and their counterions are capacitive.

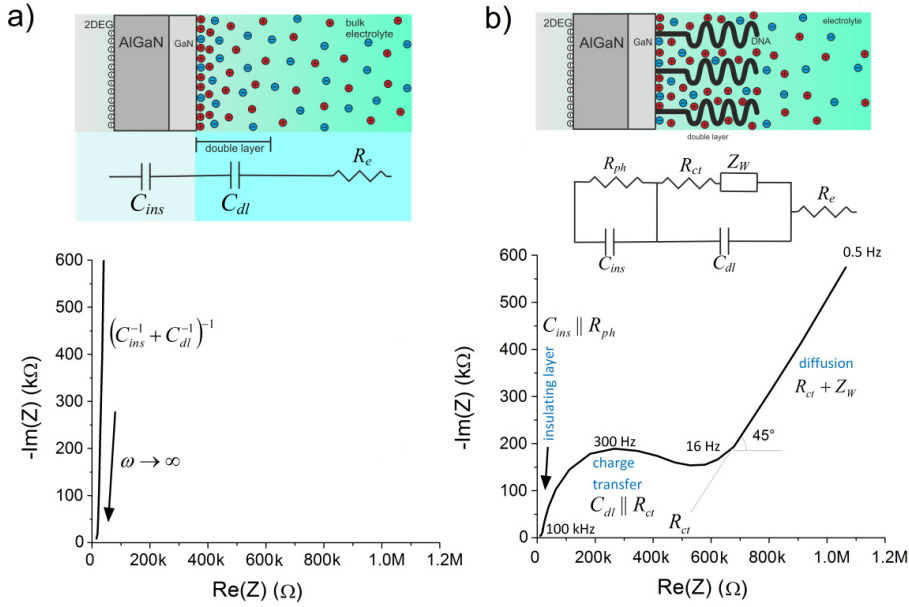


Fig. 1. Scheme of the insulator/electrolyte interface and Nyquist plot (a) prior to and (b) after functionalization. After functionalization, few pinholes appeared (R_{ph}) without affecting sensor performance. At intermediate frequencies, R_{ct} and C_{dl} (double layer capacitor) in parallel are dominant (semicircle). C_{ins} is insulator capacitance.

In electrochemistry, the impedance of a porous material is usually compared with a RC transmission line [7, 8]. The product of the resistivity and capacitance per unit length provides D . The Warburg impedance depends directly on D , D , and frequency. For a monovalent electrolyte and a diffusion length shorter than the membrane thickness, this impedance is expressed as [7]:

$$Z_W = \frac{RT}{F^2 \sqrt{2}} \left[\frac{1}{c_- \sqrt{D_-}} + \frac{1}{c_+ \sqrt{D_+}} \right] \left[\frac{1}{\sqrt{j\omega}} \right] = W \left[\frac{1}{\sqrt{j\omega}} \right] \quad (2)$$

For very high frequencies, Z_W tends to be zero. R_{ct} and W increased with target-DNA concentration (Figure 2). As probe-target is matched, the flow of electrolyte ions is reduced.

4. Dynamic detection

For very low frequencies, the circuit is approximated by $R_{ct} + Z_W$. To take benefit from the membrane impedance, a step voltage (U_{ref}) as input was applied. The bio-functionalization layer exhibits an exponential transient response, which is reflected on the normalized I_{DS} . After addition of target, this exponential behavior is slower (Figure 3a), and is related to the reduction of W/R_{ct} . The analytical solution of this approximation is very close to the measured curves (Figure 3b). An approximation for ΔI_{DS} is calculated with the inverse Laplace transform for fractional s , with application of the Mittag-Leffler function like in [9]. For the normalization, ΔI_{DS} was multiplied by R_{ct}/AU_{ref} :

$$\Delta I_{DS}(t) = A \mathcal{L}^{-1} \left\{ \frac{U_{in}(s)}{R_{ct} + Z_W(s)} \right\} = \frac{A}{R_{ct}} \mathcal{L}^{-1} \left\{ \frac{U_{ref}}{s} \frac{s^{1/2}}{s^{1/2} + \frac{W}{R_{ct}}} \right\} = \frac{AU_{ref}}{R_{ct}} \exp \left(\left(\frac{W}{R_{ct}} \right)^2 t \right) \operatorname{erfc} \left(\frac{W}{R_{ct}} t^{1/2} \right) \quad (3)$$

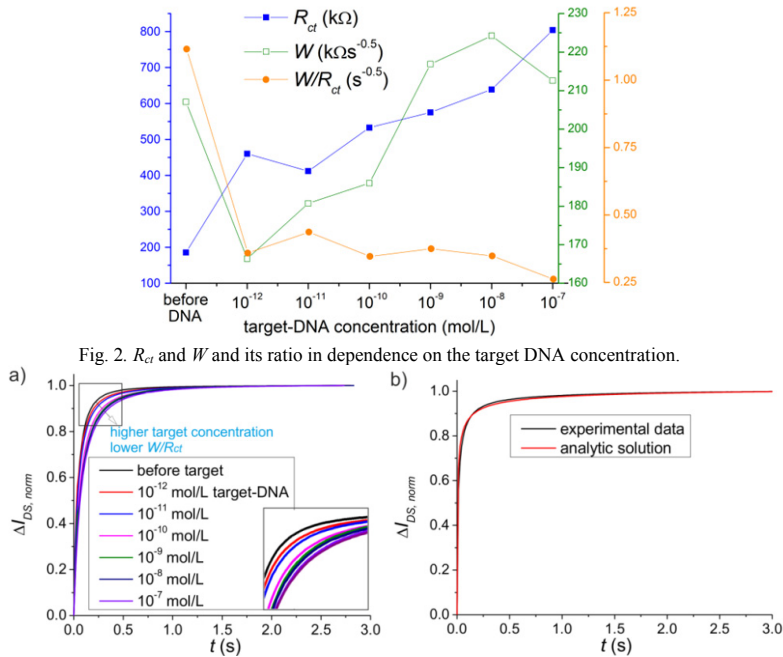


Fig. 3. (a) Dynamic response before and after target-DNA; (b) Comparison between a measured curve and analytic solution.

Conclusions and outlook

The impedimetric properties of biofilms can be employed to enhance the performance of biosensor. This approach is applicable to other kind of transistors or biosensors. Integrating $\Delta I_{DS, norm}$ (area over or under the curve) a calibration curve versus target concentration can be obtained. In future work, additional circuitry could be included to integrate $\Delta I_{DS, norm}$ in a multi-transistor array.

Acknowledgements The authors acknowledge the German Research Foundation grant GaBios (AM 105/16)

References

- [1] S. J. Pearton, et al., Recent advances in wide bandgap semiconductor biological and gas sensors, *Prog. Mater. Sci.* 55 (2010), 1-59.
- [2] S.U.Schwarz, et al., DNA-sensor based on AlGaIn/GaN high electron mobility transistor, *Phys. Status Solidi A* 208 (2011), 1626-1629.
- [3] A. Poghosian, et al., Possibilities and limitations of label-free detection of DNA hybridization with field-effect-based devices, *Sens. Actuators. B* 111-112 (2005), 470-480.
- [4] S. Ingebrandt, et. al, Label-free detection of single nucleotide polymorphisms utilizing the differential transfer function of field-effect transistors. *Biosens. Bioelectron.* 22 (2007). 2834-2840.
- [5] M. W. Shinwari, et. al, Study of the electrolyte-insulator-semiconductor field-effect transistor (EISFET) with applications in biosensor design, *Microelectron. Reliab.* 47(12) (2007), 2025-2057.
- [6] M. W. Shinwari, et. al, Analytic modelling of biotransistors, *IET Circuits Devices & Syst.* 2(1) (2008), 158-165.
- [7] I.D. Rainstrick, Chapter 2: Theory, E. Barsoukov, J.R. Macdonald (Eds.) in *Impedance spectroscopy: theory, experiment, and applications*, 2005, New Jersey, John Wiley & Sons., pp. 68-102
- [8] M. Bazant, 10.626 *Electrochemical Energy Systems* (2011), Massachusetts Institute of Technology: MIT OpenCourseWare, Lecture 35.
- [9] M. Slocinski, Modeling and parameterization, O. Kanoun (Ed.) in *Lecture Notes on Impedance Spectroscopy*. Vol. 4. 2014, London, CRC Press., pp. 3-16.